Time-of-Flight LIDAR System

Vy-An Phan
Mentor: Dr. Connie Chang-Hasnain, Adair Gerke
UC Berkeley, Integrated Optics

ABSTRACT:

We will be building a laser-based 1D distance imager, and characterizing and optimizing its performance. The goal is to surpass the range and accuracy of the current market time-of-flight LED imager (Bluetechnix Argos3D P100), which sits at approximately 5m and delivers distance reports with a 1-40% range of error depending on the reflecting surface. After the 1D distance imager is completed we can propose ways to assemble them into a coherent array of individual imagers, which can then be applied as a 3D imager.

I. Introduction

Laser ranging systems are a fairly new form of technology; however, they are easily one of the most powerful and accurate in a number of applications, especially because of their sharpness in comparison to RADAR. There exist multiple types of LIDAR setups[1]; in this paper, we will be specifically discussing a time-of-flight LIDAR system and its uses in distance measurement.

LIDAR systems operate by emitting a beam of light at a desired target and using the backscattered light to image said object. Time-of-flight LIDAR systems, in contrast to intensity-based LIDAR systems, keep track of the elapsed time between emitting and detecting a light beam. Since the speed of light is mostly constant in air, whereas the intensity of a beam can vary greatly, time-of-flight LIDAR systems are often more accurate.

Our goal is the creation of a fast and accurate time-of-flight LIDAR system, specifically, a one-dimensional distance imager. As multiple time-of-flight cameras exist on the market today, designed for various specifications[2], the target performance will be based on the range and accuracy of the current LED market imager (Bluetechnix Argos3D P100).

II. Experimental Methods

The Bluetechnix Argos3D P100 camera performed reasonably well at close, mid-range, and far distances if the target surface was diffuse. Its range is advertised as up to 5m; space constraints allowed us to test between 1-3m. Paper squares of various patterns and colors mounted on cardboard were detected between 1-6% error. However, glass and mirrors resulted in massive ranges of error, up to 44%, and were often undetectable. [Table 1]

---

[1] Berkovic, Garry; Shafir, Ehud. *Advances in Optics and Photonics* **2012**, *Vol. 4*, 442-464.
[2] Foix, Sergi; Alenya, Guillem; Torras, Carme. *IEEE Sensors Journal* **2011**, *Vol. 11*, 1-10.

Object	Real Dist. (mm)	Measured Dist. (mm)	Std. Dev.	%error
White paper	340.4	326.3	3.2	4.14%
	1051.6	1026.1	9.3	2.42%
	1762.8	1757.8	23.6	0.28%
Black paper	340.4	319.8	5.2	6.05%
	1051.6	1010.1	13.6	3.95%
	1762.8	1731.7	40.2	1.76%
Gray paper	340.4	332.5	3.0	2.32%
	1051.6	1020.6	8.7	2.95%
	1762.8	1758.6	19.3	0.24%
Red paper	340.4	335.1	2.8	1.56%
	1051.6	1019.2	7.2	3.08%
	1762.8	1758.4	18	0.25%
Green paper	340.4	339.2	3.0	0.35%
	1051.6	1019.3	7.2	3.07%
	1762.8	1756.4	17.1	0.36%
Blue paper	340.4	336.7	2.9	1.09%
	1051.6	1019.2	6.9	3.08%
	1762.8	1755.3	16.7	0.43%
Checker paper	340.4	321.1	3.5	5.67%
	1051.6	1017.1	11.4	3.28%
	1762.8	1748.7	27.4	0.80%
Glass	340.4	491.2	12.1	44.30%
	1051.6	1453.7	35.8	38.24%
	1762.8	1902.8	55.1	7.94%
Mirror	340.4	397.5	2.5	16.77%
	1051.6	1085.5	4.8	3.22%
	1762.8	1730.3	35.7	1.84%

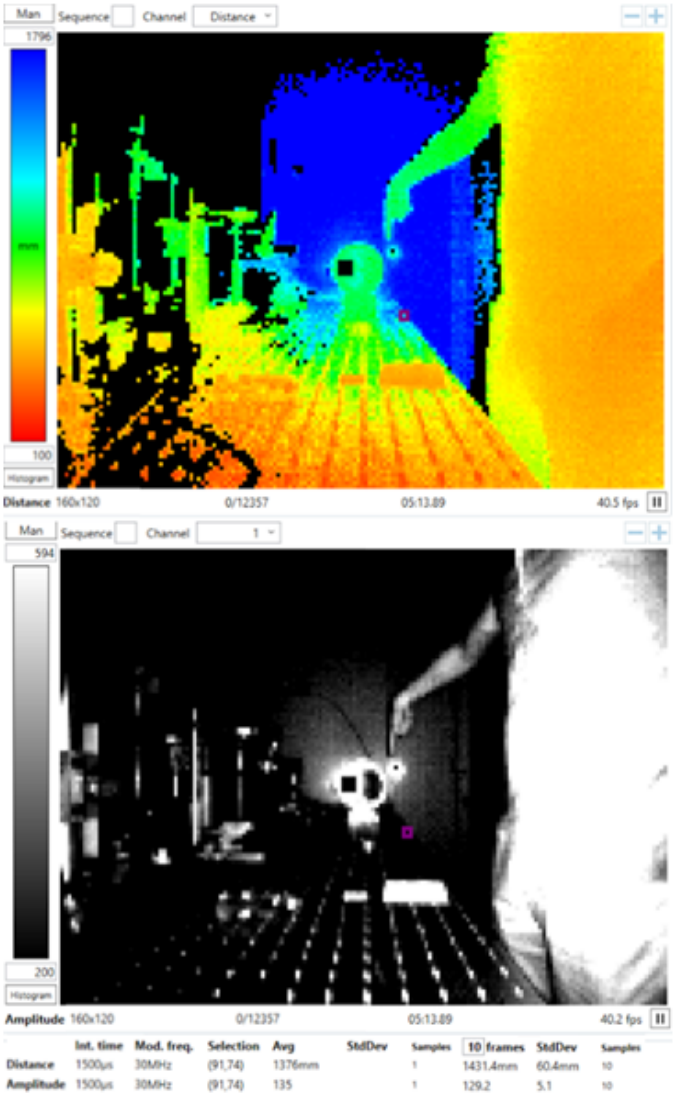

Fig. 1 (Top): Distance and amplitude measurements of a mirrored surface as seen by the Bluetechnix camera.

Table 1 (Left): Real and camera distance measurements of various surfaces. Note that for clear glass and the mirror, measurements did not always register. The error values would be much larger if we included those instances.

After testing the range and accuracy of the Bluetechnix camera, we moved on to developing our freespace LIDAR design [Fig. 2, 3]. Because of inevitable delay in both the fiber-optic and electrical cables, as well as inherent computational delay in our equipment, calculating distance from a raw time would be difficult. Therefore, we chose to set a known reference distance and base all other distance measurements on the difference in time between the reference and the target.

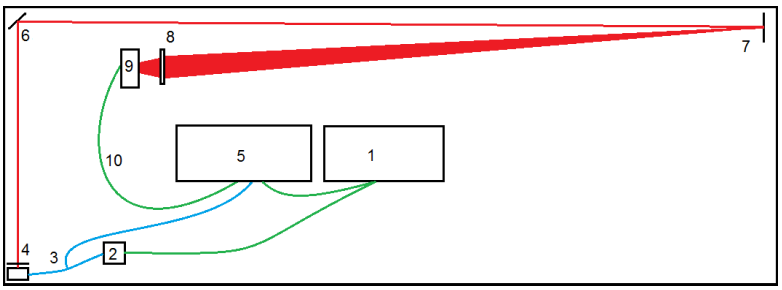

Fig. 2: A diagram of the experimental setup. The path of the laser is shown in red, electrical cabling in green, and fiber-optic cables in blue. Not pictured: Keithley, HP 6237B triple output power supply.

The signal is generated at (1) an HP 33120A function generator and fed to a (2) TO-CAN mounted 1050nm laser. The laser output is connected to a (3) 90%-10% split cable, connected to (4) a collimator and the (5) oscilloscope respectively. The sync of the (1) function generator is also connected to the oscilloscope. Meanwhile, the (4) collimator is the start of the free-space part of our freespace laser system. A (6) mirror deflects the beam around the edge of the table at the (7) imaging target. The reflected beam is focused through a (8) lens before being received by a (9) SM05PD5A photodetector, whose output is received by the (1) oscilloscope through (10) more electric cabling.

Fig. 3: Photographs of the experimental setup. Due to space constraints, we used a mirror to bend the laser beam around the corner of the table and virtually increase the maximum distance we could test.

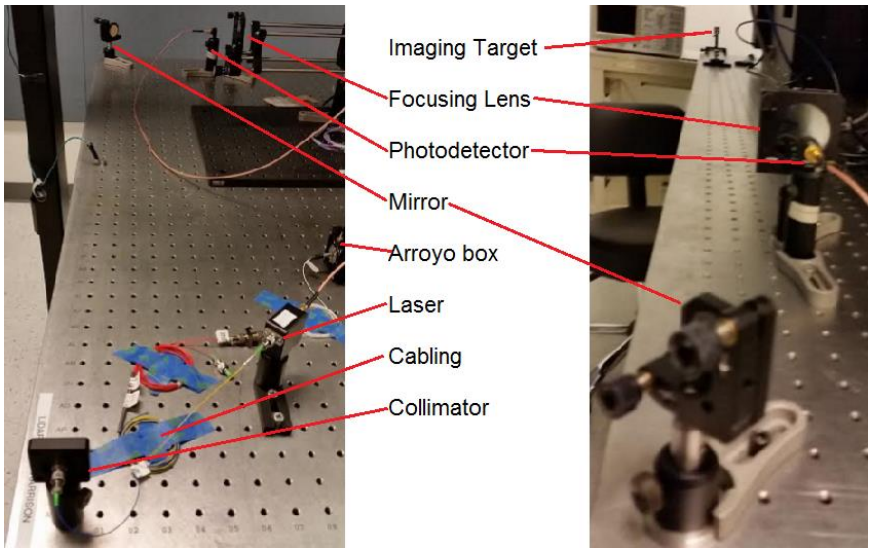

Initially, we fed a 15-MHz frequency square wave into the laser and picked two points along a set voltage threshold to find our time delay. However, because of the steep slope of the edge of the square wave, small differences on the x-axis (time) could translate to large differences on the y-axis (voltage). This caused many issues with precision, and the spread in data when using this mode of acquisition was very large. Thus, a different mode of signal processing would be needed.

We ultimately picked a sine wave as our chosen output signal for the laser, still at 15 MHz, because of its smoother time-voltage slope in comparison to the square wave. Another advantage to the sine wave was its predictable nature. Though the square wave was periodic, its edge behavior is difficult to work with because of how quickly the signal has to ramp between a zero and nonzero value. With a sine wave, however, calculating a DFT phase delay is simple enough. A third advantage is the ability of the DFT calculation to provide a continuous output

versus raw averaging, which is limited to discrete outputs because of the limited clock speed of our equipment in comparison to the natural speed of a light wave.

To collect our data, we took a series of measurements between 527 and 555cm from the front edge of the collimator at 1-cm intervals (2-cm intervals when including the round trip of the rebounded signal).

III. Results and Discussion

The ideal result of graphing real versus calculated distance would be a line of slope 1 – that is, every 1-cm change in real distance would translate to a 1-cm change in calculated distance. A constant error due to delay in the electrical wires and fiber-optic cabling is acceptable; it would simply manifest as a nonzero y-intercept, and can be easily accounted for by subtraction.

In reality, the calculated time delay, and thus the calculated distance, varied depending on the method used to extract the time delay. As stated before, the raw averaging method of extracting data provided less precise results [Fig. 4] than sine fitting [Fig. 5]. However, raw averaging ended up being more accurate, with a calculated:real distance ratio of 0.96, versus the sine fitting ratio of 0.81.

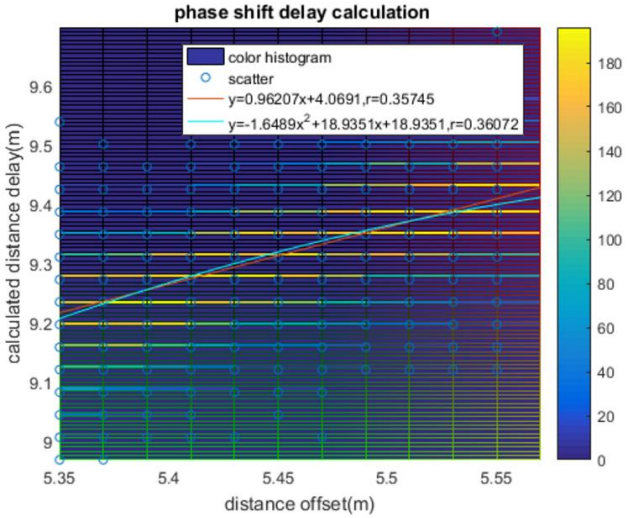

Fig. 4 (Left): Calculated vs. real distance when using raw averaging. 1000 samples were taken; the color on the heat map corresponds to the number of samples landing at a certain distance. Note the discrete values and the large spread compared to the results of the sine fitting in [Fig. 5].

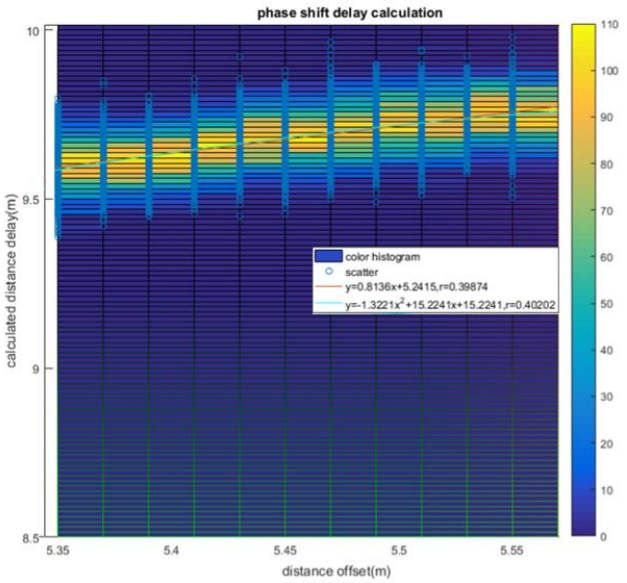

Fig. 5 (Right): Calculated vs. real distance when using raw averaging. The values are continuous and the spread is much smaller, making the answers more precise; however, the accuracy is very bad compared to the raw averaged data.

Eventually it was realized that a small sinusoidal signal was still being received even when the laser was completely covered; that is, when there should be no signal at all [Fig. 6] most likely as a leftover electromagnetic echo from the electrical cabling or within our equipment. Also, it was noted that the large error corresponded directly to a drop in voltage of the received signal [Fig. 7]. This development makes sense, as the smaller the received signal is, the more this leftover sinusoid would affect it, while a larger-amplitude signal would have an easier time drowning out the echo.

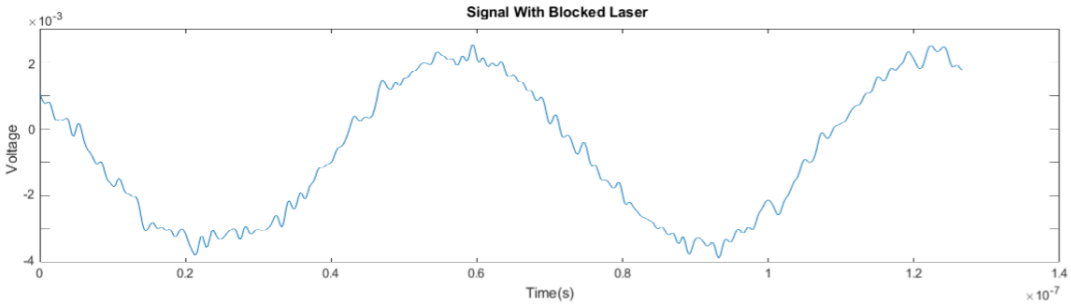

Fig. 6: A small but significant sinusoidal signal remains when the laser is covered, even though only a relatively flat line with some random noise is expected.

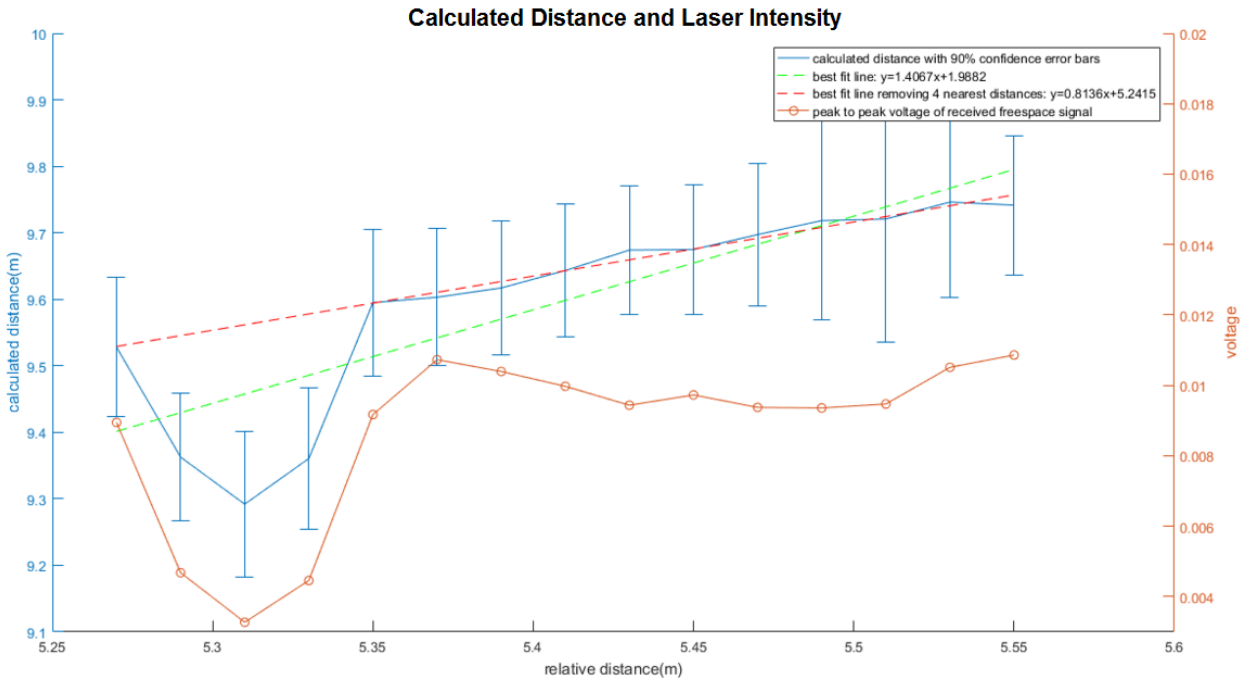

Fig. 7: The calculated versus real distance line follows a relatively straight path until the received signal from the laser dipped in amplitude. Thus it can be concluded that the source of our error is related to the strength of the received signal.

However, in either case, the echo would still be large enough to affect the overall phase of the received sinusoidal signal, throwing off the rest of the phase delay calculations.

IV. Conclusions

More work will have to be done to determine the exact sources of the echo, as well as any other potential errors. In the meantime, the error can be accounted for by collecting samples of the echo during calibration (i.e. any signals occurring when the laser is completely covered) and subtracting them out before performing the time delay calculations.

As variable modulation powers of the laser have been shown to affect the accuracy of the results with the echo in play, further tests should also be done to see if the case is still true after the residual sine wave has been removed. Tests should also be done to determine which input and output powers provide optimal results.

Finally, our LIDAR system should be tested on different surfaces other than the paper, glass, and mirrors that we used on the LED camera, such as wood, concrete, or cloth.

V. Acknowledgments

Funds for this REU research were provided by the National Science Foundation through CIAN ERC base funds, grant #EEC-0812072. Special thanks to Dr. Connie Chang-Hasnain, Harrison Hsueh, Adair Gerke, and Thai-Bao Phan.